Available online at www.sciencedirect.com
SCIENCE DIRECT®
Journal of Catalysis 220 (2003) 182–191
JOURNAL OF CATALYSIS
www.elsevier.com/locate/jcat

Palladium and platinum-based catalysts in the catalytic reduction of nitrate in water: effect of copper, silver, or gold addition

Florence Gauthard, Florence Epron,* and Jacques Barbier

Laboratoire de Catalyse en Chimie Organique (UMR6503), CNRS, Université de Poitiers, 40, Avenue du Recteur Pineau, 86022 Poitiers cedex, France

Received 25 February 2003; revised 23 May 2003; accepted 23 May 2003

Abstract

Supported bimetallic palladium and platinum catalysts promoted by metals of group 11 (Cu, Ag, and Au) were prepared by control surface deposition and tested in the liquid-phase reduction of nitrates. Whereas bimetallic catalysts promoted by gold are totally inactive, copper or silver deposition leads to bimetallic catalysts active for nitrate reduction. The promoting effect of the second metal can be related to its redox properties, confirming that nitrate reduction occurs through a bifunctionnal mechanism following (i) a direct redox mechanism between promoter and nitrate and (ii) a catalytic reaction between hydrogen, chemisorbed on the noble metal, and intermediate nitrite. TEM experiments, TPR, and FTIR of chemisorbed CO studies of the different systems have been used to evidence the metal–metal interaction and the localization of the promoter. The characterization results have been correlated with the catalytic behavior of the materials.

Keywords: Platinum or palladium based catalysts; Metals of group 11; Nitrate; Catalytic reduction

1. Introduction

Groundwater pollution by harmful nitrogen-containing compounds is a growing concern everywhere in the world. Nitrate is one of the most problematic and widespread of the vast number of potential groundwater contaminants. Sources of nitrate in groundwater can be considered in four categories: (i) natural sources, (ii) waste materials, (iii) row crop agriculture, and (iv) irrigated agriculture [1].

Biological and physicochemical treatments allow effective removal of nitrates but have several economical and ecological disadvantages. Catalytic reactions constitute promising approaches for the destruction of pollutants in water. Since the first paper of Tacke and Vorlop [2] on the use of palladium–copper bimetallic catalysts for nitrate reduction, numerous studies have been aimed at the development of suitable catalysts for the selective reduction of nitrate into nitrogen gas [2–26]. Their application in various reactor types such as suspended-bed reactor, monolithic reactor [20], hollow fibers [17], and membrane reactors [22] has been studied.

Alloying of metals may result in important changes in their activity and selectivity in catalytic reactions. As far as catalytic nitrate reduction is concerned, the changes are experimentally well established but are still not understood. Palladium catalysts have proved to be the most active and selective for nitrite reduction. However, platinum-based catalysts present an activity and a selectivity that are almost satisfactory [26]. To reduce nitrate, it is necessary to activate the precious metal by addition of a second metal of groups 11, 12, 13, or 14. Mostly, copper was used as a promoting second metal [2–26], but other suitable promoters, such as tin, indium, or zinc [5–7,17,19,21,22,25] have demonstrated interesting performances. Whereas in all cases the second metal promotes the activity, it leads to contrasting results for the selectivity.

While many studies were carried out to enhance the activity and the selectivity toward nitrogen formation, the changes in the catalytic behavior as a function of the second metal are still not fully understood and a general reaction mechanism has not been proposed yet.

Recently, the behavior of platinum catalysts promoted by copper deposition has been studied for nitrate reduction in the liquid phase [26]. The proposed mechanism involves a redox reaction between metallic copper and nitrate, leading to intermediate nitrite or directly to nitrogen gas or ammo-

* Corresponding author.
E-mail address: florence.epron.cognet@univ-poitiers.fr (F. Epron).

0021-9517/$ – see front matter
doi:10.1016/S0021-9517(03)00252-5

nium ion, and to an oxidized form of copper. In this way, the role of the precious metal is to activate hydrogen, allowing the reduction of oxidized copper to prevent deactivation. Concerning intermediate nitrite, it can be reduced either on copper according to a redox reaction or on precious metal by a catalytic reaction.

With the aim of gaining a deeper understanding of the reaction mechanism, we have studied the effect of the promoter on the activity and selectivity of platinum and palladium-based catalysts. For that purpose, metals of group 11 (Cu, Ag, Au) have been chosen.

Generally, bimetallic catalysts are prepared either (i) by loading the support simultaneously with both metal precursors (deposition–precipitation or impregnation) or (ii) by modifying a parent monometallic catalyst by impregnating the promoter precursor (successive impregnation). Under these conditions, the promoter is randomly deposited on the support and/or on the noble metal. Previous studies [26,27] showed that controlled surface reactions (catalytic reduction or direct redox reaction) constitute a way of catalyst preparation bringing the two metals in close contact, with a specific orientation of the second metal deposit on the first one, which is different from classical methods described above. Moreover, in the case of Pt-Cu/γ-Al_2O_3 bimetallic catalysts, it was demonstrated that the preparation methods involved different behaviors in nitrate abatement. Precisely, the preparation method by catalytic reduction led to the most active catalysts compared to those resulting from classical methods such as coimpregnation or successive impregnation [26].

This paper describes the performance for nitrate and nitrite removal and characteristics of various bimetallic catalysts, supported on alumina, involving a metal of group 11 and prepared by catalytic reduction. The characteristics of mono and bimetallic particles were studied by temperature-programmed reduction (TPR), infrared spectroscopy (FTIR) of chemisorbed CO, transmission electron microscopy (TEM) coupled with energy dispersive spectrometry (EDS) and H_2 chemisorption. They were tentatively related to metal–metal interactions, resulting from the preparation steps, and to the catalytic activity for nitrate reduction.

2. Experimental

2.1. Catalyst preparation

2.1.1. Monometallic catalysts

A powdered γ-alumina from Procatalyse (surface area (BET method), 216 m^2/g; pore volume, 0.55 m^3/g; isoelectric point, 7) has been used as support. First, it was ground and then sieved to retain particles with sizes between 0.04 and 0.08 mm.

Monometallic catalysts were prepared by an impregnation method using aqueous solutions of the precursor salts: $Pd(NH_3)_4(NO_3)_2$ and $Pt(NH_3)_4(OH)_2$. This step consisted of a cationic exchange between the precursor salt and the alumina surface possible at high pH. After evaporation of water, catalysts were dried at 120 °C, calcinated in flowing air at 450 °C for 4 h, and reduced by flowing hydrogen at 500 °C for platinum and 300 °C for palladium.

Monometallic catalysts Pt/γ-Al_2O_3 and Pd/γ-Al_2O_3 had a metal loading of 3 wt% and 1.6 wt%, respectively. These two different metal loadings correspond to equimolar quantities of the precious metal. In the following, these catalysts are identified by their respective notation: Pt3Al and Pd1.6Al.

2.1.2. Bimetallic catalysts

Bimetallic catalysts were prepared by a controlled surface reaction. In order to obtain great metal–metal interactions, the second metal was deposited by a redox reaction occurring between the hydrogen adsorbed on the prereduced noble metal and the oxidized modifier.

A known amount of a monometallic catalyst was placed in an atmospheric glass reactor. The reactor was flushed with a countercurrent nitrogen flow for 15 min at room temperature. Afterward the catalyst was reduced by a hydrogen stream at a temperature rising to 400 °C and then cooled to room temperature. At the same time, the desired amount of the modifier was predissolved in water and degassed by bubbling with N_2. The solution was then added to the monometallic catalyst and maintained under stirring by hydrogen flow for 2 h. The bimetallic catalyst was separated from the aqueous solution via a filter in the bottom of the reactor, and washed. Therefore, the resulting material was dried overnight under a nitrogen stream at 70 °C.

Each bimetallic catalyst, made up of a precious metal (M) and a promoter (X), was identified by its specific atomic ratio x (at.%) in the metallic phase corresponding to the number of atoms of X divided by the total number of atoms (M + X). The catalyst was noted MX_xAl.

The experimental nominal composition of each catalyst was verified by elementary analysis. Generally, the experimental value gave an incertitude error not exceeding 5%.

2.2. Characterization methods

2.2.1. Metal accessibility

H_2 chemisorption measurements were carried out using a conventional volumetric apparatus equipped with a turbomolecular pump. Prereduced samples were reduced again in flowing hydrogen at their reduction temperature. Then, they were outgassed at this temperature until a vacuum below 1 Pa was achieved, in order to obtain metal free of hydrogen, and after that cooled to room temperature. Hydrogen chemisorption was conducted at room temperature for platinum catalysts, whereas it was operated at 70 °C for palladium catalysts to avoid the formation of β-PdH [28,29]. The linear portions of both the total and the reversible chemisorption isotherms were extrapolated to zero pressure to estimate the corresponding uptakes. The fraction of exposed noble

metal atom was taken as $(H/M)_{irr}$, assuming that the surface stoichiometry of the irreversibly adsorbed hydrogen is unity.

2.2.2. TEM measurements

TEM measurements were carried out with a Philips CM120 electron microscope operating at 120 kV with a resolution of 0.35 nm. The powder was ultrasonically dispersed in ethanol, and the suspension was deposited on an aluminum grid coated with a porous carbon film. The particle-size distribution was obtained from TEM pictures calculating the surface average particle diameter from $d_p = \sum n_i d_i^3 / \sum n_i d_i$.

X-ray energy dispersive spectrometry (EDX) was performed with the STEM mode of the microscope using a Si-Li Super UTW detector.

2.2.3. FTIR spectroscopy

Spectra were recorded on a Perkin-Elmer spectrometer from Nicolet in the 4000–1000 cm^{-1} range with a resolution set at 4 cm^{-1}. Samples were pressed in order to obtain thin disks which were directly introduced in the IR cell and subjected to different thermal and chemical treatments, namely outgassing and reduction. The spectrum of the reduced sample was used as the reference and the plot function was set in absorbance mode.

The catalysts were reduced in flowing hydrogen at the reduction temperature for 1 h (500 °C for platinum and 300 °C for palladium) and evacuated at the same temperature for 1 h in order to remove adsorbed hydrogen over the surface of metal particles. Carbon monoxide was introduced in the cell at room temperature by injecting pulses until saturation of the metal surface. Then, the samples were evacuated at room temperature for 1 h. The spectra presented in the present study were obtained by difference between the absorbance of the sample measured under vacuum before and after adsorption of the probe molecule.

2.3. Nitrate and nitrite reduction

Nitrate and nitrite reduction reactions were performed in a semibatch reactor, at atmospheric pressure and 10 or 25 °C. In a typical experiment, 200 mg of the powdered catalyst, with a particle diameter between 40 and 80 µm, was placed in 90 ml of ultrapure water (18.2 MΩ), purged with nitrogen and then with hydrogen. Afterward, 10 ml of a solution (16 mmol L^{-1}) of nitrate (KNO_3 or $Mg(NO_3)_2$) or nitrite (KNO_2 or $Ba(NO_2)_2$) was introduced in the reactor to start the reaction. The catalyst dispersion in the aqueous medium was achieved by the hydrogen flow ($p_{H_2} = 1$ bar, flow rate = 250 ml min^{-1}) through a porous glass located at the bottom of the reactor. To monitor the progress of the reaction, representative aqueous samples were periodically withdrawn and immediately separated by filtration and then analyzed as described in Section 2.4.

Catalysts were compared as a function of their initial activity, corresponding to the initial disappearance rate of nitrite or nitrate, and of their selectivity toward ammonium ions, determined at the end of the reaction.

2.4. Analysis

The reaction components were analyzed by the HPLC method. Nitrate and nitrite concentrations were determined after separation on a Zorbax Eclipse XDB-C18 column using an UV detector at $\lambda = 210$ nm. Ammonium ions were quantified using an Alltech Universal cation column coupled with a conductivity detector. The acidic mobile phase (oxalic acid) used provided the complete conversion of the ammonia basic form into ammonium ions.

3. Results and discussion

3.1. Monometallic catalysts

The metal accessibility of the monometallic catalysts, Pt/γ-Al_2O_3 and Pd/γ-Al_2O_3, was determined immediately after preparation (fresh catalyst) and also after a blank test (i.e., under flowing hydrogen in water) in order to discriminate between the modifications induced by the preparation conditions of the bimetallic catalyst and the actual effect of the second metal. A sintering phenomenon occurred in water under hydrogen flowing which was expressed by a decrease of the metal accessibility determined by hydrogen volumetric chemisorption: from 61 to 52% for Pt/γ-Al_2O_3 and from 80 to 13% for Pd/γ-Al_2O_3. So the catalytic performances for nitrite reduction were determined after ageing in water under flowing hydrogen. Catalytic properties and particle size of the monometallic catalysts are summarized in Table 1. These results demonstrate that the platinum activity is lower and its selectivity toward ammonium ions is higher compared to palladium. These results are quite in agreement with the first investigations reported in the literature [3]. The lower selectivity toward ammonium ions of monometallic palladium could be explained by the less noble character of palladium compared with that of platinum, that is, unfavorable to the deep reduction of nitrogen species into ammonium ions. This selectivity difference could also

Table 1
Initial activity and final selectivity toward ammonium ions for nitrite reduction,[a] and particle size of platinum and palladium catalysts supported on alumina

Monometallic catalyst	Metal loading (wt%)	d (Å)[b]	d (Å)[c]	TOF (10^{-3} s^{-1})	Selectivity (mol%)
Pt3Al	3	16	19	29	67
Pd1.6Al	1.6	72	59	230	39

[a] Nitrite source, $Ba(NO_2)_2$; reaction temperature, 25 °C.
[b] Average particle size after ageing in water under hydrogen flow determined by H_2 chemisorption.
[c] Average particle size after ageing in water under hydrogen flow determined by TEM.

Table 2
Redox potentials of metals of group 11 and principal nitrogen species involved in the reaction as intermediates or final products [30,31]

Redox systems	E^0 (V/ERH)
Cu^{2+}/Cu	0.34
Ag^{+}/Ag	0.799
Au^{3+}/Au	1.52
NO_3^-/NO_2^-	0.835
NO_3^-/NH_4^+	0.88
NO_3^-/N_2	1.25

be explained by the difference of particle size of the two monometallic catalysts (see 3.2.2.2b).

3.2. Bimetallic catalysts

3.2.1. Pd-Au/γ-Al_2O_3 catalyst

Two Pd-Au/γ-Al_2O_3 catalysts were prepared from the parent catalyst Pd1.6Al containing 10 and 50 at.% of gold in the bimetallic phase. The catalytic experiments performed in the presence of these materials demonstrated that Pd-Au/γ-Al_2O_3 is inactive for nitrate reduction. This could be explained by the inability of gold to reduce nitrate by a direct redox process, according to the redox potentials of the Au^{3+}/Au couple (Table 2) and of the possible nitrogen species involved in the reaction. This hypothesis was confirmed by testing a monometallic 10 wt.% Au/γ-Al_2O_3 catalyst after an in situ prereduction, which was totally inactive for nitrate as well as for nitrite reduction under nitrogen or hydrogen atmosphere. The inactivity toward nitrite reduction under hydrogen could be surprising since gold has a higher noble character than palladium, but it cannot chemisorb hydrogen at ambient temperature [32] that could account for this result.

3.2.2. Bimetallic catalysts promoted by copper or silver addition

Contrary to gold, the addition of copper or silver to Pt3Al and Pd1.6Al leads to active catalysts for nitrate and nitrite reduction. In the following, Pt–Ag, Pt–Cu, Pd–Ag, and Pt–Cu catalysts will be characterized by TPR, FTIR, TEM, and XRD and then their activity and selectivity for nitrate and nitrite reduction will be examined.

3.2.2.1. Characterization Pt–Ag, Pt–Cu, Pd–Ag, and Pt–Cu supported on alumina with a same atomic ratio of promoter in the metal phase (50 at.%) were characterized by TPR, FTIR of adsorbed CO, and TEM coupled with EDS. Their respective notation are the following: PtAg50Al, PtCu50Al, PdAg50Al, and PdCu50Al.

3.2.2.1.a. TPR. Temperature-programmed reduction profiles of bimetallic catalysts were established after preparation and exposition to air at ambient temperature (fresh catalyst). Indeed, it was demonstrated that an oxidation at high temperature of a bimetallic catalyst can lead to the segregation of the two metals [33].

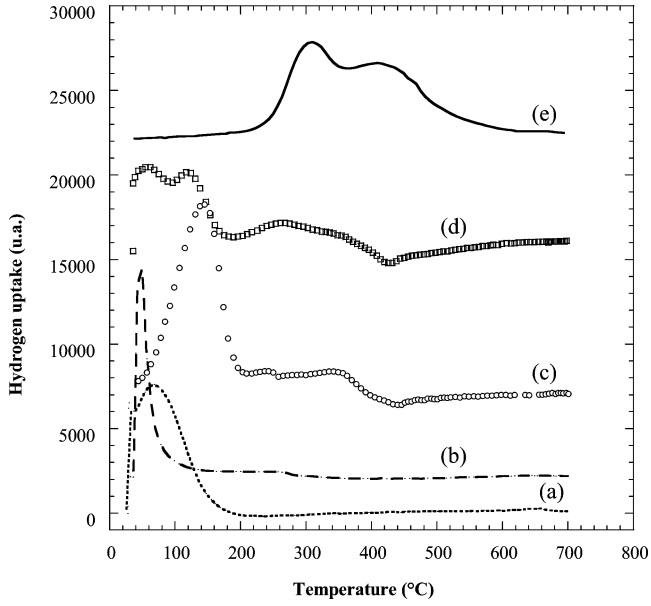

Fig. 1. TPR profiles of γ-Al_2O_3-supported monometallic catalysts and their corresponding bimetallic promoted by copper addition: (a) oxidized Pt3Al, (b) oxidized Pd1.6Al, (c) fresh PtCu50Al, (d) fresh PdCu50Al, and (e) oxidized Cu1Al.

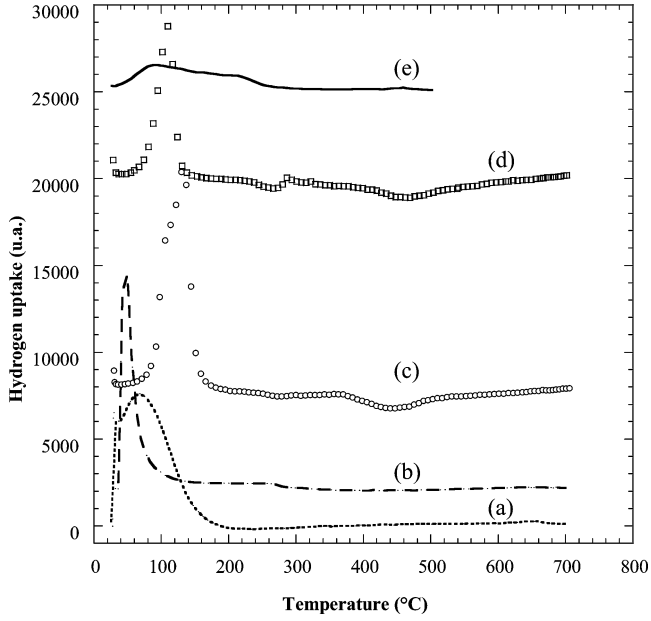

Fig. 2. TPR profiles of γ-Al_2O_3-supported monometallic and their corresponding bimetallic catalysts promoted by silver addition: (a) oxidized Pt3Al, (b) oxidized Pd1.6Al, (c) fresh PtAg50Al, (d) fresh PdAg50Al, and (e) oxidized Ag1.7Al.

The TPR profiles of the bimetallic catalysts were compared to those of the corresponding monometallic catalysts determined after oxidation under air at 400 °C (Figs. 1 and 2). The temperatures of the maximum hydrogen uptake rate (T_M) for the different metal oxides are listed in Table 3.

The TPR profiles of the oxidized Pt3Al (Fig. 1, a) and Pd1.6Al (Fig. 1, b) catalysts show a hydrogen consumption from ambient temperature and are characterized by a sin-

Table 3
Temperature (T_M) at the maximum of reduction rate for alumina-supported monometallic catalysts

Metal oxides	T_M (°C)
PdO_x	~25
PtO_x	70
CuO	310
Cu_2O	420
AgO	~100
Ag_2O	~200

gle peak. Concerning 1 wt% Cu/γ-Al_2O_3 catalyst, named Cu1Al, (Fig. 1, e), its profile is characterized by a hydrogen consumption at higher temperature with two peaks at 300 and 400 °C. These peaks could be respectively assigned to superficial Cu_2O and CuO reduction to metallic copper [33]. In the case of 1.7 wt% Ag/γ-Al_2O_3, named Ag1.7Al, (Fig. 2, e), the TPR profile is composed of two peaks at 110 and 220 °C, corresponding to the reduction of AgO and Ag_2O [34].

As far as the TPR profiles of bimetallic catalysts are concerned (Figs. 1 and 2), they all present an important hydrogen consumption whereas they were not preoxidized at high temperature, that underlines a nonnegligible oxidation of the bimetallic catalysts at ambient temperature.

On the TPR profile of the PtCu50Al catalyst (Fig. 1, c), an important hydrogen uptake around 150 °C followed by a slight hydrogen uptake between 250 and 400 °C is identified. The first reduction peak situated between those of pure platinum and copper catalysts indicates the reduction of mixed Pt–Cu oxidized species where both metals are in close contact. The peak at higher temperatures could be attributed to oxidized copper species not interacting with the platinum.

From the TPR profile of PdCu50Al catalyst (Fig. 1, d), one can observe an important hydrogen consumption characterized by two maximum temperatures (at $T_M = 75$ and 135 °C) and a wide hydrogen consumption between 200 and 400 °C. The first reduction peaks at 75 and 135 °C are shifted toward higher temperatures compared to monometallic palladium catalyst, demonstrating the presence of an interaction between palladium and copper in the metallic particles. The hydrogen consumption from 200 °C results from the reduction of isolated copper particles as it has been already observed for PtCu50Al catalyst.

Considering now the TPR profiles of catalysts promoted by silver PtAg50Al and PdAg50Al reported in Fig. 2, only one peak of thermoreduction is identified, located at a higher temperature than that of the corresponding pure noble catalyst. Therefore, it may be assumed that this peak corresponds to the coreduction of both metals.

All the TPR profiles of the different bimetallic catalysts have proved the presence of metal–metal interaction. It leads one to suppose that bimetallic entities are present in all these bimetallic catalysts. This result is rather satisfying since the preparation method favors the deposition of the promoter preferentially onto the noble metal particles.

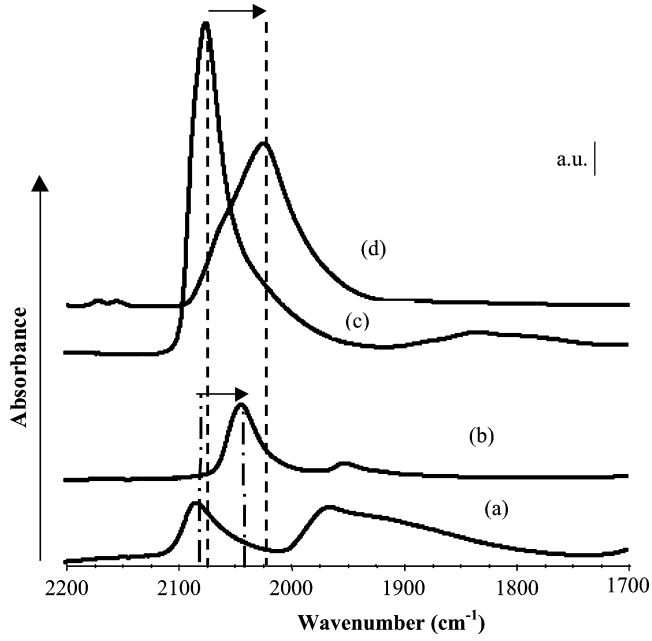

Fig. 3. FTIR spectra of CO adsorbed at room temperature onto monometallic Pt3Al and Pd1.6Al and bimetallic PtAg50Al and PdAg50Al catalysts (after saturation of the surface with CO followed by evacuation for 1 h at room temperature): (a) Pd1.6Al, (b) PdAg50Al, (c) Pt3Al, (d) PtAg50Al.

3.2.2.1.b. FTIR. Infrared spectroscopy of chemisorbed CO was principally used in order to determine the location of the promoter onto the noble metal particles. This study was carried out by comparing IR spectra of freshly prepared bimetallic catalysts and blank monometallic catalysts, that means treated in water under hydrogen flow. On Fig. 3 are seen the IR spectra of the bimetallic catalysts promoted by silver and of the monometallic parent catalysts. The IR spectrum recorded on the blank Pd1.6Al catalyst (Fig. 3, a) shows two main peaks of adsorbed CO in the 1750–2150 cm^{-1} range. The band at ca. 2085 cm^{-1} corresponds to linearly bound adsorbed CO while the band at ca. 1950 cm^{-1} is attributed to bridged CO [35,36]. Otherwise, the IR spectrum of the blank Pt3Al catalyst (Fig. 3, c) is composed of only one band at 2070 cm^{-1} which is characteristic of linear CO species [37], the bridged form of CO adsorbed onto platinum (near 1850 cm^{-1}) being negligible [38]. The comparison of the different IR spectra points out that the deposition of silver onto the monometallic Pd1.6Al and Pt3Al catalysts leads to a shift to lower wavenumbers of the stretch frequency of CO adsorbed on the noble metal. This result bears out that the silver deposit induces an effect of dilution of the particles of precious metal. In other words, it indicates an interaction between the noble metal and the promoter into the bimetallic catalysts. The infrared spectra of the monometallic catalysts modified by the addition of copper have the same profile that also underlines the presence of interactions between both species of the metallic phase.

In accordance with previous works, the spectra corresponding to the CO adsorption on Pd and Pt monometallic catalysts can be decomposed into five elementary adsorp-

tion bands in the case of palladium crystallites [39,40] and only three elementary bands for platinum [41]. The carbonyl bands of adsorbed CO on the noble metal were deconvoluted using spectra adjustment software (Peakfit). The deconvolution of the ν_{CO} bands was realized assuming each elementary adsorption band as a gaussian curve. Knowing the surface of each elementary band forming the IR spectra for all catalysts, the contribution to the total absorbance of the two types of adsorption of CO (linear noted L and bridged noted B) can be calculated for each palladium-based catalyst. Whereas linear species L are mainly considered to correspond to CO adsorbed on low coordinated palladium atoms (edges, corners etc.), the bridged species B are situated on Pd(100) or Pd(110) and on Pd(111) [42–45]. Results, reported in Table 4, show that for palladium-based catalysts the proportion of linear species is increased when Cu or Ag is added to the detriment of the bridged species compared to the monometallic palladium-supported catalyst. This phenomenon appears independently of the nature of the second metal, although it is more pronounced in the case of silver. Moreover, this behavior is in accordance with the one we could attempt considering the preparation method, the "catalytic reduction," which favors the deposition of the second metal (Cu or Ag) onto the precious metal (Pd). Consequently, the probability of the presence of two adjacent sites able to adsorb carbon monoxide as bridged species is decreased. This indicates that the deposition of the promoter could occur preferentially on the terrace sites.

For platinum-based catalysts only the linear species are quantified. Results, reported in Table 4, demonstrate that apparently copper induces a weak variation of the quantity of sites suitable for absorption of carbon monoxide as linear species corresponding to the edge and corner sites of platinum crystallites. This effect is not observed for the catalyst modified by silver, that could evidence different deposition sites depending on the second metal. The method used to deposit the second metal onto the noble metal by catalytic reduction could account for this different behavior. This method consists of a surface redox reaction between chemisorbed hydrogen and the second metal according to the overall reaction:

$$n H_{ads} + X^{n+} \rightarrow X_{ads} + n H^{+},$$

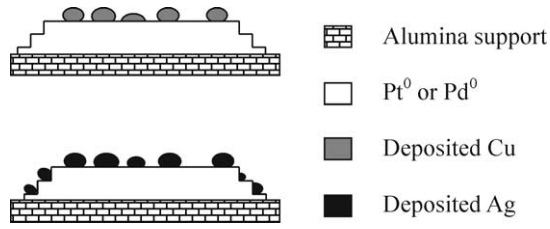

Fig. 4. Schematic representation of the localization of the promoter on the palladium or platinum particle according to the FTIR results.

where H_{ads} is adsorbed hydrogen on the precious metal (Pt or Pd), M^{n+} is cation of the second metal, and M_{ads} is adsorbed second metal.

Since the silver precursor is a monovalent cation whereas the one of copper is bivalent, it can be assumed that the preferential sites for the second metal deposit are different. Indeed, copper requires two hydrogen atoms chemisorbed on adjacent metallic sites to be deposited whereas the deposition of silver presents no constraint. Therefore, copper could be preferentially deposited on the terrace sites whatever the nature of the noble metal, as schematized on Fig. 4. This type of deposit could lead to the creation of defects on the surface of the noble metal, which would contribute to the adsorption of CO as linear species instead of bridged species. As far as silver is concerned, it could be deposited on the terrace sites as well as on the edge and corner sites of the crystallites of platinum or palladium (Fig. 4).

3.2.2.1.c. TEM and EDX. TEM pictures coupled with EDS were carried out to collect more information about the homogeneity of the particles in terms of particle size and of composition. The TEM pictures and particle-size distributions of the four different bimetallic catalysts (PtCu50Al, PdCu50Al, PtAg50Al, and PdAg50Al) are illustrated in Figs. 5 and 6, respectively.

If we refer to the particle size of the monometallic catalysts (Table 1), we can see that the average particle sizes of the monometallic parent catalysts are practically not modified by the addition of copper, whereas the deposition of silver leads to an important increase of the average diameters. Moreover, the comparison of the particle-size distributions (Fig. 6) demonstrates that bimetallic catalysts containing silver are heterogeneous with sizes varying between 10 and around 200 nm.

Table 4
Surfaces (L and B) and ratio (L/(L+B)) of the IR bands corresponding to bridged and linearly bonded CO on monometallic catalysts (Pt and Pd) and bimetallic catalysts (Pt-X and Pd-X with X = Ag or Cu)

Catalyst	Linear carbonyl species L		Bridged carbonyl species B		Surface ratio
	Frequency ($\bar{\nu}$)	Surface (a.u.)	Frequency ($\bar{\nu}$)	Surface (a.u.)	L/(L+B)
Pd1.6Al	2083	0.34	1965	3.48	0.089
PdCu50Al	2065	0.36	1981	0.90	0.286
PdAg50Al	2043	1.12	1951	0.28	0.800
Pt3Al	2075	8.3	–	–	–
PtCu50Al	2060	10.6	–	–	–
PtAg50Al	2025	8.1	–	–	–

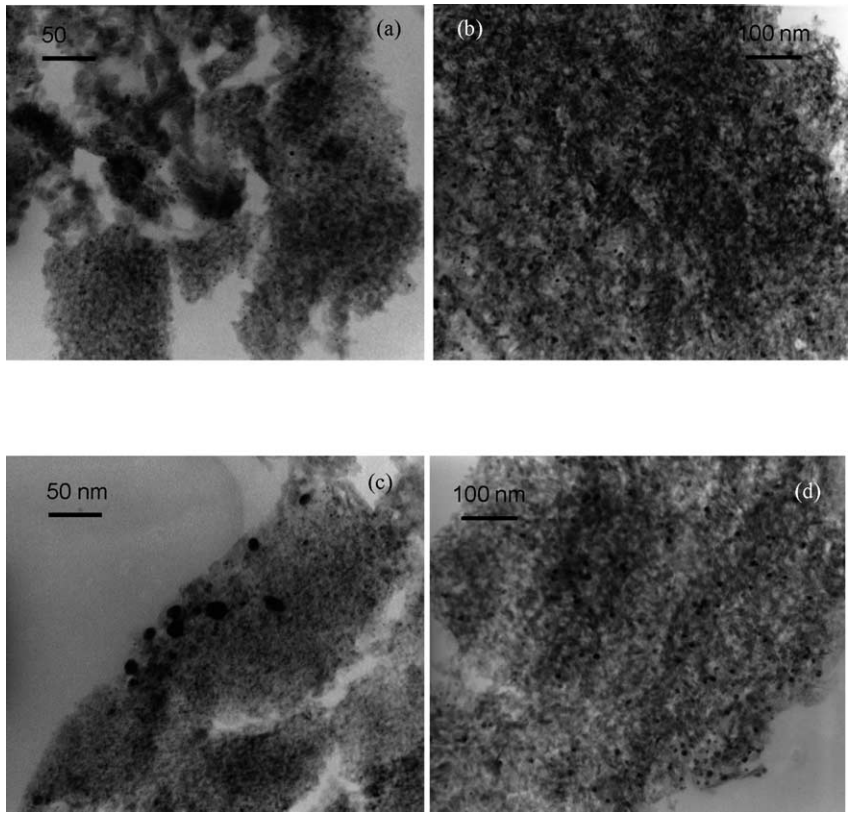

Fig. 5. TEM pictures of (a) PtCu50Al, (b) PdCu50Al, (c) PtAg50Al, and (d) PdAg50Al.

EDX analysis has demonstrated that the composition of around 80% of the analyzed individual particles corresponds to the average composition of the whole catalyst, except for PtAg50Al. For this catalyst, bimetallic particles were composed either of 20 at.% or of 80 at.% of Ag, and some monometallic silver particles were found isolated on the support.

3.2.2.2. Nitrate reduction It is well known that copper is a good promoter for nitrate reduction whereas in the case of silver, published investigations have reported a weak activity. In Fig. 7 are displayed the evolution of nitrate and intermediate nitrite concentrations in the presence of PdCu50Al and PdAg50Al. This figure underlines that, contrary to the results of the literature, silver-promoted noble metal catalysts can have a higher activity than classical copper-promoted catalysts, when bimetallic catalysts are prepared by catalytic reduction. As the redox potential of the Ag^+/Ag couple is lower than that of nitrogen species involved in the reaction, we can suggest that, according to our previous proposed mechanism [26,46] metallic silver is able to reduce nitrate yielding to nitrite formation. As we have demonstrated that silver is deposited on the noble metal, that is favored by the preparation method, the enhancement of the activity of the present Pd–Ag catalyst compared to the results of the literature could be explained by the ability of the noble metal to maintain silver in the metallic state under hydrogen.

With the aim of gaining a deeper understanding of this type of catalytic system, the influence of the promoter content on the catalytic properties was studied for four types of catalysts, Pt–Ag, Pt–Cu, Pd–Ag, and Pd–Cu supported on alumina.

3.2.2.2.a. Effect of promoter content in the metal phase on the activity. The promoter content in the bimetallic catalysts was varied, maintaining constant the precious metal loading (0.15 mmol/g_{cat}). The activities of the different bimetallic catalysts are presented in Fig. 8 as a function of the promoter proportion in the bimetallic phase. This figure shows that, for both types of noble metal-based catalysts, the activity for nitrate reduction appears to go through a maximum for a promoter content between 33 and 50 at.%, depending on the catalyst. The optimal composition and the corresponding activity are reported in Table 5 as a function of the bimetallic catalyst. Except for the bimetallic PdCuAl catalyst, for which the maximum of activity is reached for 33 at.% of copper, in agreement with results of the literature [3,26], the optimal content of the promoter is 50 at.% in the bimetallic phase. The maximum of activity of the four bimetallic systems is quite the same, between 0.13 and 0.19 mmol of nitrate converted per minute and gram of catalyst. This maximum of activity is reached when the optimal concentrations of bimetallic entities, made up of a promoter, able to reduce nitrate, and of a noble metal, able to activate hydrogen to maintain the promoter in the metallic state, are simultaneously present in the catalyst. In conclusion, the cata-

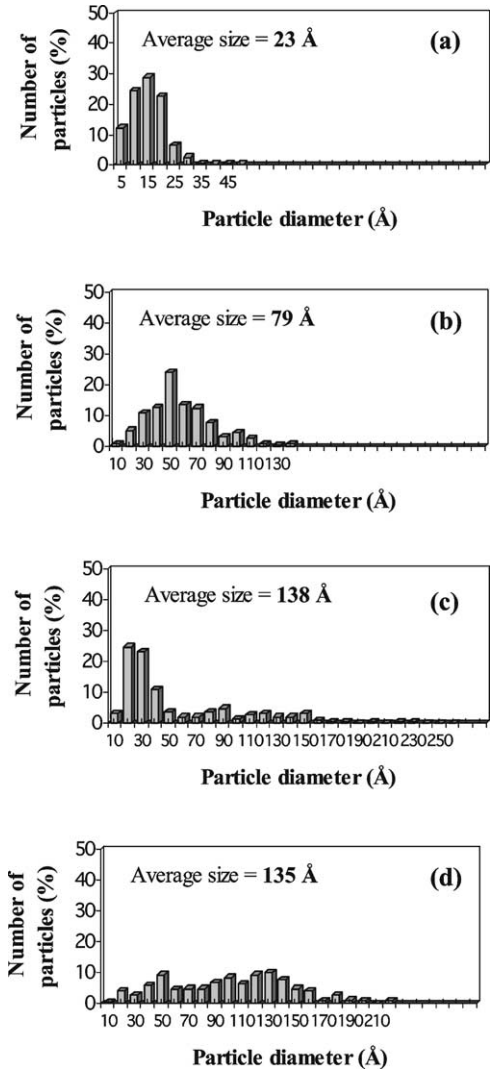

Fig. 6. Histograms of particle sizes of (a) PtCu50Al, (b) PdCu50Al, (c) PtAg50Al, and (d) PdAg50Al determined from TEM pictures.

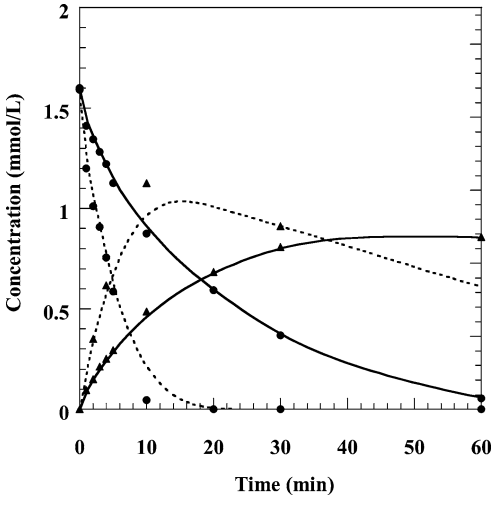

Fig. 7. Nitrate (●) and nitrite (▲) concentration vs time in the presence of PdCu50Al (—) or PdAg50Al (- - -) catalysts ($T = 10\,^{\circ}$C, nitrate source $Mg(NO_3)_2$).

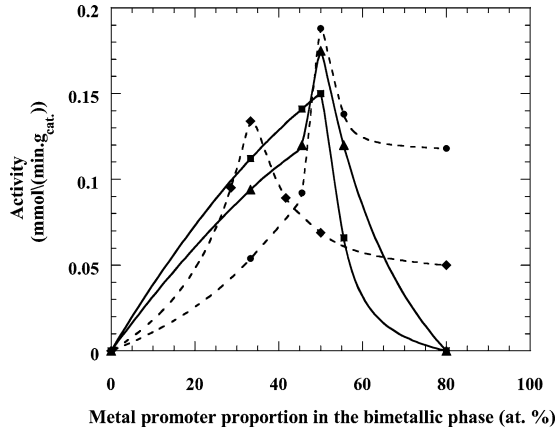

Fig. 8. Initial activity for nitrate reduction as a function of the promoter content in the metal phase (X/(M + X) at.%) for bimetallic catalysts promoted by copper or silver: PtCuAl (●), PtAgAl (■), PdCuAl (◆), and PdAgAl (▲) ($T = 10\,^{\circ}$C, nitrate source $Mg(NO_3)_2$).

Table 5
Initial activity and final selectivity toward ammonium ions of bimetallic catalysts (Pt-X and Pd-X with X = Ag or Cu) with the optimal composition for nitrate reduction ($T = 10\,^{\circ}$C, nitrate source $Mg(NO_3)_2$)

Catalyst	Promoter content (at.%)	Activity (mmol/(min g_{cat}))	Selectivity (%)
PtCuAl	50	0.19	75
PdCuAl	33	0.13	60
PtAgAl	50	0.15	65
PdAgAl	50	0.17	56

lysts leading to the higher activity are PtCu50Al, PdCu33Al, PtAg50Al, and PdAg50Al.

3.2.2.2.b. Selectivity toward ammonium ions. The selectivity toward ammonium ion formation was determined for the four optimized catalysts PtCu50Al, PdCu33Al, PtAg50Al, and PdAg50Al. Results are reported in Table 5. According to this table, bimetallic catalysts show high selectivities toward ammonium ions, 56 to 75% of nitrate being reduced into ammonium ions, depending on the noble metal and the promoter.

Several parameters could explain (i) the high selectivities and (ii) the slight differences in selectivities as a function of the bimetallic catalysts. It has been demonstrated that the pH in the vicinity of the active sites strongly affects the selectivity toward ammonium ions [6,12,47,48]. Consequently, as hydroxide ions are produced during nitrate and nitrite reduction, the porosity of the support and the pH of the solution during the reaction play a role of major importance in the ammonium ion formation. In the present study, nitrate reduction was performed without pH control and the same value of pH 11 was reached at the end of the reaction. Then, the pH of the solution can explain the high selectivities toward ammonium ions, observed for all the catalysts. On the other hand, the same support, a γ-alumina with a BET surface of 215 m^2/g and a total pore volume of 0.55 cm^3/g, was used to prepare all the catalysts and it was verified that the porosity is not affected by the addition of the metals. Then the

Table 6
Initial activity of monometallic catalysts (Pt and Pd) and bimetallic catalysts (Pt-X and Pd-X with X = Ag or Cu) for nitrite reduction ($T = 10\,^{\circ}C$, nitrite source $Ba(NO_2)_2$)

Catalyst	Promoter content (at.%)	Activity (mmol/(min g_{cat}))
Pt3Al	–	0.04
Pd1.6Al	–	0.060
PtCuAl	50	0.058
PdCuAl	50	0.061
PtAgAl	50	0.02
PdAgAl	50	0.032

differences of selectivities, as a function of the bimetallic catalysts, cannot be related to the porosity. Other parameters such as the particle size, the electronic, and/or by a geometric effect induced by the promoter could explain these changes.

3.2.2.3. Nitrite reduction Nitrite reduction was performed in the presence of the four bimetallic systems Pt–Ag, Pt–Cu, Pd–Ag, and Pt–Cu supported on alumina, containing the same atomic ratio of the promoter (50 at.% in the bimetallic phase). Their activity, compared with that of the monometallic equivalents, is reported in Table 6. Contrary to the reduction of nitrate, the reduction of nitrite proceeds rapidly on monometallic catalysts. The activity of bimetallic catalysts demonstrates that the reaction rate is slightly increased by the addition of copper, whereas it is strongly decreased by the addition of silver. This difference of activity, probably due to the inactivity of silver for nitrite reduction contrary to copper, explains the higher intermediate nitrite concentration during nitrate reduction in the case of silver as promoter (see Fig. 8). Moreover, for a given promoter, modified $Pd/\gamma\text{-}Al_2O_3$ catalysts show higher activity than modified $Pt/\gamma\text{-}Al_2O_3$ catalysts. This is consistent with the activity of the parent monometallic catalysts ($Pd/\gamma\text{-}Al_2O_3$ and $Pt/\gamma\text{-}Al_2O_3$) for nitrite reduction.

4. Conclusion

The modification of a parent monometallic $Pd/\gamma\text{-}Al_2O_3$ or $Pt/\gamma\text{-}Al_2O_3$ catalyst by deposition of metal of group 11 (Cu, Ag, Au) using the preparation method called catalytic reduction leads to bimetallic catalysts with high metal–metal interactions, as proved by TPR and TEM coupled with EDX and FTIR. As a function of the promoter, the characterization by FTIR of adsorbed CO and by TEM coupled with EDX has revealed different morphologies. The addition of copper leads to homogeneous bimetallic particles with a narrow size distribution, copper being deposited selectively on terrace sites. On the contrary, the deposition of silver is made at random on all types of sites.

Gold deposition on a precious metal leads to bimetallic catalysts inactive for nitrate reduction. On the other hand, silver is a good promoter for this reaction, bimetallic catalysts having an activity of the same order as those containing copper. The promoting effect of these metals can be related to their ability to reduce nitrate according to a redox reaction under the conditions of the reaction. Gold, which is nobler than palladium or platinum, is not able to achieve this process, contrary to silver and copper. Then, the proposed mechanism for nitrate reduction onto $Pt\text{-}Cu/\gamma\text{-}Al_2O_3$ catalysts [26] can be generalized to whole systems associating a noble metal and an oxidizable promoter.

In conclusion, the present study confirms that nitrate reduction occurs according to a bifunctionnal mechanism involving a direct redox mechanism on the promoter followed by a classical catalytic reaction on the noble metal. A system active for nitrate reduction is necessarily composed of (i) one promoter easily oxidizable and reducible in the reaction conditions and (ii) one noble metal able to chemisorb hydrogen.

Acknowledgment

F.G. gratefully acknowledges La Région Poitou-Charentes for research fellowships.

References

[1] L.W. Canter, Nitrates in Groundwater, CRC Press, Boca Raton, FL, 1996.
[2] T. Tacke, K.-D. Vorlop, Dechema Biotechnology Conferences, Vol. 3, VCH, Weinheim, 1989, p. 1007.
[3] S. Hörold, T. Tacke, K.D. Vorlop, Environ. Technol. 14 (1993) 931.
[4] S. Hörold, K.D. Vorlop, T. Tacke, M. Sell, Catal. Today 17 (1993) 21.
[5] U. Prüsse, S. Hörold, K.-D. Vorlop, Chem.-Ing.-Tech. 69 (1997) 93.
[6] U. Prüsse, M. Hahnlein, J. Daum, K.D. Vorlop, Catal. Today 55 (2000) 79.
[7] U. Prüsse, J. Daum, C. Bock, K.D. Vorlop, Stud. Surf. Sci. Catal. 130 (2000) 2237.
[8] U. Prüsse, K.-D. Vorlop, J. Mol. Catal. 173 (2001) 313.
[9] A. Pintar, J. Batista, J. Levec, T. Kajiuchi, Appl. Catal. B 11 (1996) 81.
[10] A. Pintar, M. Setinc, J. Levec, J. Catal. 174 (1998) 72.
[11] A. Pintar, J. Batista, J. Levec, Water Sci. Technol. 37 (1998) 177.
[12] A. Pintar, J. Batista, Catal. Today 53 (1999) 35.
[13] A. Pintar, J. Batista, J. Levec, Chem.-Eng.-Sci. 56 (2001) 1551.
[14] A. Pintar, J. Batista, J. Levec, Catal. Today 66 (2001) 503.
[15] F. Deganello, L.F. Liotta, A. Macaluso, A.M. Venezia, G. Deganello, Appl. Catal. B 24 (2000) 265.
[16] O.M. Ilinitch, L.V. Nosova, V.V. Gorodetskii, V.P. Ivanov, S.N. Trukhan, E.N. Gribov, S.V. Bogdanov, F.P. Cuperus, J. Mol. Catal. A 158 (2000) 237.
[17] M. Hählein, U. Prüsse, J. Daum, V. Morawsky, M. Kröger, M. Schröder, M. Schnabel, K.-D. Vorlop, in: B. Delmon, et al. (Eds.), Preparation of Catalysts, Vol. VIII, Elsevier, Amsterdam, 1998, p. 99.
[18] G. Strukul, F. Pinna, M. Marella, L. Meregalli, M. Tomaselli, Catal. Today 27 (1996) 209.
[19] G. Strukul, R. Gavagnin, F. Pinna, E. Modaferri, S. Perathoner, G. Centi, M. Marella, M. Tomaselli, Catal. Today 55 (2000) 139.
[20] J. Wärna, I. Turunen, T. Salmi, T. Maunula, Chem. Eng. Sci. 49 (1994) 576.
[21] A.J. Lecloux, Catal. Today 53 (1999) 23.

[22] K. Daub, G. Emig, M.-J. Chollier, M. Callant, R. Dittmeyer, Chem.-Ing.-Sci. 54 (1999) 1577.
[23] H. Berndt, I. Mönnich, B. Lücke, M. Menzel, Appl. Catal. B 30 (2001) 111.
[24] Y. Yoshinaga, T. Akita, I. Mikami, T. Okuhara, J. Catal. 207 (2002) 37.
[25] L. Lemaignen, C. Tong, V. Begon, R. Burch, D. Chadwick, Catal. Today 75 (2002) 43.
[26] F. Epron, F. Gauthard, C. Pinéda, J. Barbier, J. Catal. 198 (2001) 309.
[27] C. Micheaud, P. Marecot, M. Guerin, J. Barbier, Appl. Catal. A 171 (1998) 229.
[28] V. Ragiani, R. Giannantonio, P. Magni, L. Lucarelli, G. Leofanti, J. Catal. 146 (1994) 116.
[29] H. Berndt, J. Dembowski, K. Flick, Chem. Technol. 49 (1997) 12.
[30] M. Pourbaix, N. de Zoubov, Atlas d'équilibres électrochimiques à 25 °C, Gauthier-Villars, Paris, 1963.
[31] J.T. Maloy, in: A.J. Bard, R. Parsons, J. Jordan (Eds.), Standard Potentials in Aqueous Solution, Dekker, New York, 1985, p. 127.
[32] R. Culver, J. Pritchard, F.C. Tompkins, Proc. 2nd Int. Congr. Surf. Act. 2 (1957) 243.
[33] F. Epron, F. Gauthard, J. Barbier, Appl. Catal. A 237 (2002) 253.
[34] Q. Zhang, J. Li, X. Liu, Q. Zhu, Appl. Catal. A 197 (2000) 221.
[35] R.P. Eischens, W.A. Pliskin, Adv. Catal. 10 (1958) 1.
[36] L.L. Sheu, Z. Karpinski, W.M.H. Sachtler, J. Phys. Chem. 93 (1989) 4890.
[37] N. Sheppard, Y.T. Nguyen, in: R.J.H. Clark, R.E. Hester (Eds.), Infrared and Spectroscopy, Vol. 5, Books Demand, Ann Arbor, MI, 1978, p. 67.
[38] A. Palazov, C.C. Chang, R.J. Kokes, J. Catal. 36 (1975) 338.
[39] C. Binet, A. Jadi, J.C. Lavalley, J. Chim. Phys. 86 (1989) 451.
[40] C. Binet, A. Jadi, J.C. Lavalley, J. Chem. Soc. Farad. Trans. 88 (1992) 2079.
[41] R.G. Greenler, K.D. Burch, Surf. Sci. 152/153 (1985) 338.
[42] R.F. Hicks, Q.J. Yen, A.T. Bell, J. Catal. 89 (1984) 498.
[43] V. Pitchon, M. Primet, H. Praliaud, Appl. Catal. 62 (1990) 317.
[44] J. Evans, B.E. Hayden, G. Lu, Surf. Sci. 360 (1996) 61.
[45] L.F. Liotta, G.A. Martin, G. Deganello, J. Catal. 164 (1996) 322.
[46] F. Epron, F. Gauthard, J. Barbier, J. Catal. 206 (2002) 363.
[47] U. Prüsse, V. Morawsky, A. Dierich, A. Vaccaro, K.-D. Vorlop, in: B. Delmon, et al. (Eds.), Preparation of Catalysts, Vol. VII, Elsevier, Amsterdam, 1998, p. 137.
[48] R. Gavagnin, L. Biasetto, F. Pinna, G. Strukul, Appl. Catal. B 38 (2002) 91.